M_2L_6 Complexes with Triple Mo−Mo and W−W Bonds: Molecular Topology and Inverted Pyramidality Effect

Xiang-Yang Liu and Santiago Alvarez*

Departament de Química Inorgànica, Universitat de Barcelona, Diagonal 647, 08028 Barcelona, Spain

Received October 10, 1996[⊗]

A molecular orbital study of the model compounds $[Mo_2(NH_2)_6]$, $[Mo_2(OH)_6]$, $[W_2H_6]$ and $[W_2Cl_6]$, indicates that the M−M bond strength should increase with increasing pyramidality (i.e., the average of the M−M−L bond angles) up to a certain angle (the turnover point), after which the trend is inverted. The topology of the metal-centered π-type orbitals of the ML_3 fragments favors the appearance of the turnover point at a smaller angle than the minimum in energy, resulting in an inverted pyramidality effect for the experimentally attainable angles. A structural database search supports the theoretical findings: the M−M distances in triple-bonded complexes of d^3 transition metal ions in the families $[Mo_2(NR_2)_6]$, $[W_2(NR_2)_6]$, and $[W_2(OR)_6]$ decrease with increasing pyramidality angles, while the $[Mo_2(OR)_6]$ complexes present a parabolic bond distance−bond angle dependence.

The preparation and study of transition-metal complexes with multiple metal−metal bonds have received considerable attention in the past decades.[1,2] The most common compounds of this type are those with the M_2L_{2n} ($n = 3$ or 4) stoichiometry. One of the essential geometrical parameters of the M_2L_8 system is the "pyramidality" of its ML_4 fragments, defined by the average of the M−M−L angles (α in **1**). It has been found

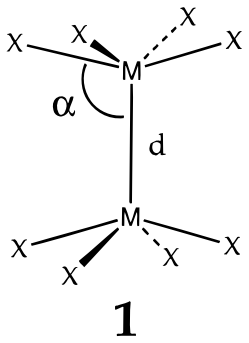

1

that the metal−metal bond distances depend not only on bond order and steric effects but also on the pyramidality, as confirmed by the analysis of structural data from different systems with M−M single,[3] triple, or quadruple[4,5] bonds. Even for dimers of d^8 square-planar complexes with metal−metal contacts has a clear pyramidality effect been found.[6]

A general description of the pyramidality effect in metal−metal bonded-systems is given by a parabolic dependence of the M−M bond distance on the pyramidality (Figure 1): as the α increases, the M−M bond distance decreases, eventually reaching a minimum, after which further increase in α results in an elongation of the M−M distance. In practice, only a small fraction of the $d(\alpha)$ curve is energetically attainable, and the

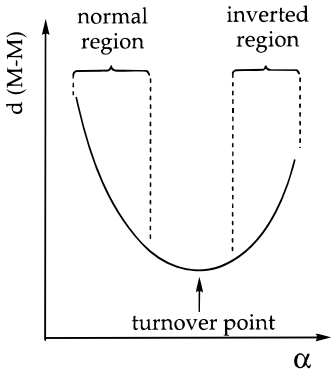

Figure 1. Schematic representation of the three regions in which can be divided the general parabolic dependence of the M−M bond length on the pyramidality α for the binuclear compounds M_2L_n.

available structural data correspond in general to one of three possible situations: (a) the *normal* region (small values of α), in which *d* is roughly a linear function of α with a negative slope, (b) the turnover point, around which *d* is practically independent of α (intermediate α values), and (c) the *inverted* region (large values of α) in which *d* is approximately a linear function of α with a positive slope. For only a few families do the experimental data cover a range of pyramidalities sufficiently wide to make the parabolic behavior evident.[5]

The experimental control of the pyramidality effect could be a useful tool in designing new compounds with desired properties. For instance, it would allow bond dissociation to be favored by forcing small values of α. On the contrary, one could envisage to stabilize elusive M−M bonds by appropriately choosing the adequate degree of pyramidalization.[4] In binuclear complexes of paramagnetic metal ions, the magnetic coupling could be made more ferromagnetic or antiferromagnetic by adequately varying the degree of pyramidalization. Finally, changes in the energy of the highest occupied and lowest unoccupied molecular orbitals associated with changes in the degree of pyramidalization should allow one to fine-tune the optical properties of binuclear complexes.

To extend our systematic study of the pyramidality effect to different types of compounds, we have focused on the d^3−d^3 triple-bonded binuclear compounds of general formula M_2L_6, where M = Mo, W and L = NR_2 or OR. This family of

[⊗] Abstract published in *Advance ACS Abstracts*, February 15, 1997.

(1) Cotton, F. A.; Walton, R. A. *Multiple Bonds Between Metal Atoms*, 2nd ed.; Oxford University Press: Oxford, U.K., 1993.
(2) Chisholm, M. H. *Acc. Chem. Res.* **1990**, *23*, 419.
(3) Aullón, G.; Alvarez, S. *Inorg. Chem.* **1993**, *32*, 3712.
(4) Losada, J.; Alvarez, S.; Novoa, J. J.; Mota, F.; Hoffmann, R.; Silvestre, J. *J. Am. Chem. Soc.* **1990**, *112*, 8998.
(5) Mota, F.; Novoa, J. J.; Losada, J.; Alvarez, S.; Hoffmann, R.; Silvestre, J. *J. Am. Chem. Soc.* **1993**, *115*, 6216.
(6) Aullón, G.; Alemany, P.; Alvarez, S. *Inorg. Chem.* **1996**, *35*, 5061.

S0020-1669(96)01235-9 CCC: $14.00

compounds provides us with valuable information on some of the topological factors that determine the position of the turnover point, thus providing some insight into possible ways to predetermine a normal or inverted pyramidality effect. A qualitative molecular orbital analysis is presented, based on extended Hückel (EH) calculations, which is verified by means of density functional (DFT) calculations. Then the experimental data for the M_2L_6 compounds are studied in a search for structural correlations between the M−M bond distances and the pyramidality α. Finally, comparison of both the experimental and theoretical results for the Mo_2L_8 and Mo_2L_6 families provides a simple explanation for the anomalous pyramidality effect of the latter.

Orbital Effects of Pyramidalization of ML_n Fragments

We start by a qualitative analysis of what should be expected on the basis of the topologies of the molecular orbitals of two interacting ML_n fragments. If we were able to understand the evolution of the overlap between the metal-centered fragment orbitals with the pyramidality, we should be able to explain the changes in metal−metal bond strength and the associated changes in metal−metal bond distances. For the present qualitative discussion we use two interacting ML_4 fragments as a model, because their high symmetry makes them a convenient starting point. It can be easily shown that the qualitative ideas can be applied to the ML_3 fragments which are the object of the present study. Later on, the discussion of subtle differences found when the two interacting fragments are ML_3 will provide new insight on the different behavior of M_2L_6 and M_2L_8 complexes.

A general principle that proves to be very helpful in the present context is that the metal-centered fragment orbitals are always hybridized in such a way as to become as less M−L antibonding as possible, i.e., increasing their density in directions away from the ligands. We start by looking at the case of σ-donor only ligands, using as a model $[W_2H_8]^{2-}$. In the planar ML_n group, d_{z^2} mixes with the metal s orbital, reducing its density in the molecular plane (where the M−L antibonding character is concentrated) and increasing it in the out-of-plane regions. As that fragment is pyramidalized, the ligands move toward the nodal cone of d_{z^2}, thus decreasing the need for such hybridization (**2a**). One should therefore expect that the overlap

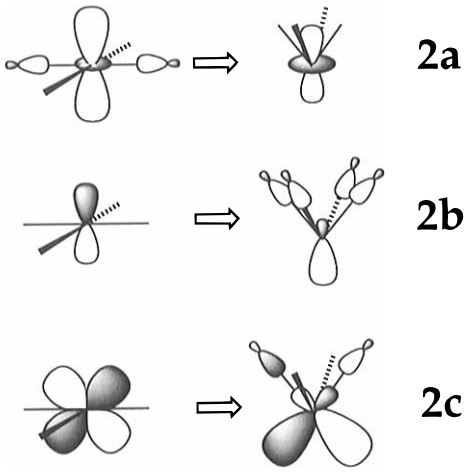

between the d_{z^2} orbitals of the two ML_n fragments decreases as their planarity is lost (i.e., with increasing pyramidality), as seen in Figure 2 (top). On the other hand, the overlap between d_{z^2} in one metal atom and p_z in the other atom improves with pyramidality for $\alpha \simeq 90°$, given the increased hybridization of p_z (**2b**), and this interaction has been shown to be important in determining the susceptibility to pyramidalization of compounds

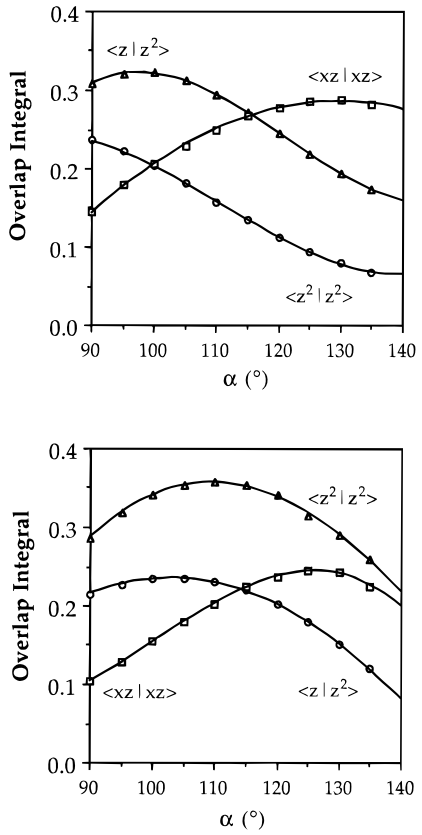

Figure 2. Dependence of the overlap integrals between fragment molecular orbitals (FMO's) on the pyramidality in the model compounds $[W_2H_8]$ (top) and $[W_2Cl_8]$ (bottom), calculalted at the EH level. The overlap integrals represented are those between the FMO's with a major contribution from the p_z metal orbital in one fragment and d_{z^2} in the other one (triangles); d_{z^2} and d_{z^2} (circles) and d_{xz} with d_{xz} (squares).

with single Rh(II)−Rh(II) bonds.[3] At larger angles, dehybridization of d_{z^2} (**2a**) is the prevailing effect and the $\langle d_{z^2}|p_z\rangle$ overlap integral decreases with α (Figure 2, top). As a result of the two combined overlaps, the σ metal−metal bond is little sensitive to pyramidalization at small angles.

If one considers now the π M−M bonding, the interaction between the fragment orbitals built mostly from the metal d_{xz} and d_{yz} atomic orbitals must be analyzed. These fragment orbitals increase their hybrid character upon pyramidalization (**2c**). Since the maximum overlap with the σ-donor orbitals of the ligands results at $\alpha = 135°$, the maximum hybridization (hence the stronger metal−metal π-bonding) should be expected at that angle. The calculations on the model compound with σ-only-donor hydrides clearly confirm this simple picture (Figure 2, top). The presence of π-donor ligands somewhat modifies the pyramidality dependence of the σ and π metal−metal interactions, as seen for the analogous model with chloride ligands (Figure 2, bottom). For example, when the ligands are displaced out of the molecular plane, the d_{z^2} orbital mixes in an antibonding way with the p_π orbitals of the ligand, favoring its hybridization as indicated in **3**, thus favoring a stronger σ overlap with increasing pyramidality.

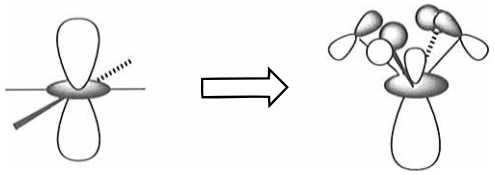

3

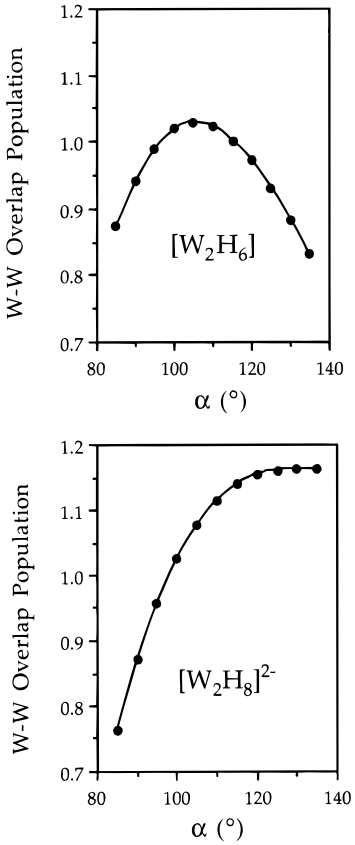

Figure 3. Calculated M−M overlap population (EH) plotted as a function of the pyramidality α for the model complexes $[W_2H_6]$ (top) and $[W_2H_8]^{2-}$ (bottom).

Theoretical Study of Pyramidality in M_2L_6 Complexes

Theoretical studies of electronic structure and bonding in M_2L_6 complexes have been previously reported,[7−11] so we refer to these papers for a qualitative discussion of the molecular orbitals, metal−metal bonding, photoelectron spectra, and bond energies. However, the interrelationship between bond angle and bond length in this family of compounds has not been previously studied from a theoretical point of view.

In Figure 3 we show the calculated W−W overlap population in the model compounds $[W_2H_6]$, together with that for $[W_2H_8]^{2-}$ for comparison. There it can be seen that substituting ML_3 fragments for the ML_4 ones has an important effect on the bond angle dependence of the bond strength. For small angles, an increase in the pyramidality strengthens the M−M bond, just as in the M_2L_8 case discussed above. However, a maximum is reached after which the opposite effect is observed: the M−M bond is weakened as the pyramidality increases.

Before trying to find an explanation for the parabollic pyramidality behavior predicted for the M_2L_6 complexes, and for the fact that the turnover point appears at smaller angle than in the analogous M_2L_8 compounds, we verified our qualitative reasoning by performing DFT calculations (see Appendix for details) for M_2L_6 complexes, using $[Mo_2(OH)_6]$ and $[Mo_2(NH_2)_6]$ as models for the series of alkoxo and amido complexes. For the sake of comparison, we report also calculations for $[Mo_2(OH)_4(NH_2)_2(NH_3)_2]$ as representative of the family of triple-bonded Mo_2L_8 complexes. Keeping the M−L distances frozen, we optimized the Mo−Mo distance for every pyramidality angle (α). The energy minima in the resulting two-dimensional potential energy surface correspond to α = 102.9°, d = 2.308 Å for $[Mo_2(OH)_6]$ and α = 102.5°, d = 2.256 Å for $[Mo_2(NH_2)_6]$.

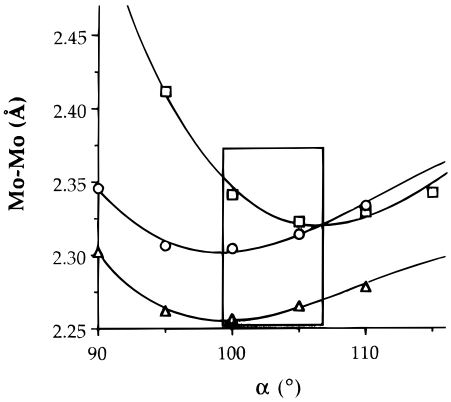

Figure 4. Optimized M−M bond distances (DFT) as a function of the pyramidality α for the triple-bonded compounds $[Mo_2(NH_2)_6]$ (triangles), $[Mo_2(OH)_6]$ (circles), and $[Mo_2(OH)_4(NH_2)_2(NH_3)_2]$ (squares). The outline shows the range of structures with energies within 5 kcal/mol above the minima.

The optimized Mo−Mo distances for $[Mo_2(OH)_6]$ and $[Mo_2(NH_2)_6]$ (Figure 4) present the parabolic dependence on α sketched in Figure 1. One must consider that substituent effects, steric interligand interactions, or intermolecular interactions with counterions or solvation molecules can force pyramidality angles different than that found as the most stable in our model calculations. Hence, we may arbitrarily consider as observable only those angles with energies 5 kcal/mol above the minimum at most. For $[Mo_2(OH)_6]$ and $[Mo_2(NH_2)_6]$, we are left with those values of α between 98 and 108°. Within that range, the calculated distances are approximately linear on α, with an inverted pyramidality effect.

We go back now to a qualitative model, in an attempt to provide a rationale for the different behavior of the M_2L_6 and M_2L_8 families of compounds. Such difference is ultimately tied to the different symmetry of the fragments involved: C_{4v} and C_{3v} for the ML_4 and ML_3 groups, respectively. We recall that, in M_2L_8, the orbitals of the ML_4 group participating in the metal−metal π bond (2e) are increasingly hybridized toward the second ML_4 group when α increases (**2c**). Hence, the overlap between the π-type orbitals increases with α, resulting in increasing d_{xz}/d_{xz} and d_{yz}/d_{yz} overlap populations (Figure 5, bottom), presumably reaching a maximum at α ≈ 135°. The related effect on the σ M−M bond is much smaller (Figure 5), as expected from the qualitative analysis above. The combined effect of the pyramidality on σ and π M−M bonds nicely corresponds to the variation of the total M−M overlap population calculated at the EH level (Figure 3) and to the variation of the calculated M−M distances at the DFT level (Figure 4).

The fact that the turnover point appears in the M_2L_6 complexes at smaller angles than in the M_2L_8 analogues is probably responsible for the fact that the inverse pyramidality effect is observed in the former (see below), while a direct effect is most common among the latter.[5] Thus, it is interesting to find the reason for such a difference. In the M_2L_6 molecule, the π orbitals of each ML_3 fragment are d_{xz} and d_{yz} (2e in the C_{3v} symmetry group). For a planar ML_3 fragment (α = 90°), as happens for ML_4, these orbitals cannot mix with other metal atomic orbitals. As the fragment is pyramidalized (α > 90°), they can mix with d_{xy} and $d_{x^2-y^2}$ (3e) and with p_x and p_y (4e).

(7) Dedieu, A.; Albright, T. A.; Hoffmann, R. *J. Am. Chem. Soc.* **1979**, *101*, 3141.
(8) Ziegler, T. *J. Am. Chem. Soc.* **1983**, *105*, 7543.
(9) Bursten, B. E.; Cotton, F. A.; Green, J. C.; Seddon, E. A.; Stanley, G. G. *J. Am. Chem. Soc.* **1980**, *102*, 4579.
(10) Hall, M. B. *J. Am. Chem. Soc.* **1980**, *102*, 2104.
(11) Kok, R. A.; Hall, M. B. *Inorg. Chem.* **1983**, *22*, 728.

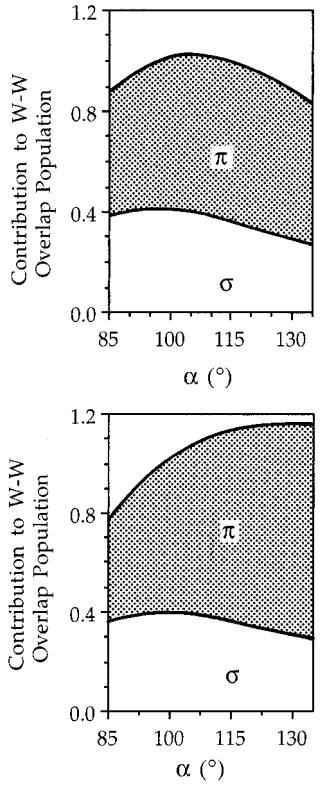

Figure 5. σ and π contributions to the M−M overlap population as a function of the pyramidality α for the model complexes with triple M−M bonds $[W_2H_6]$ (top) and $[W_2H_8]^{2-}$ (bottom).

The effect of mixing with the p orbitals is the same as that discussed above for the ML_4 fragments (**4a**), but further mixing

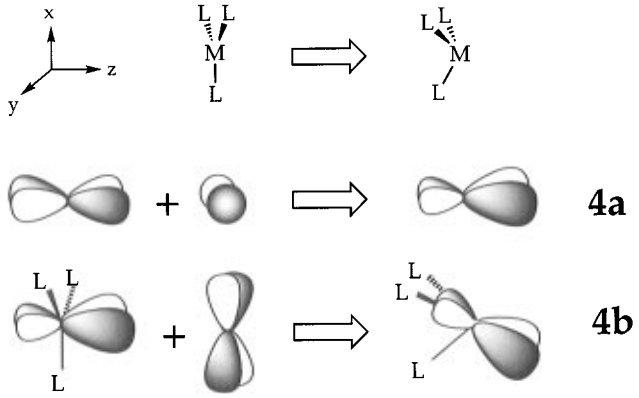

with d_{xy} and $d_{x^2-y^2}$ results in a tilting of the 2e orbitals away from the W−W direction[12] (**4b**), in an attempt to become as little M−L antibonding as possible. To analyze the π bonding, one needs now to consider the interaction not only between the 2e orbitals of each fragment but also between 2e and 3e. The evolution of the corresponding overlap integrals as a function of α is shown in Figure 6. As could be expected from the topology of these orbitals, the 2e/2e overlap decreases with increasing α, due to the increased tilting, but at small angles this is compensated by an increase in the 2e/3e overlap. The 2e/2e and 2e/3e overlap populations evolve in the same way

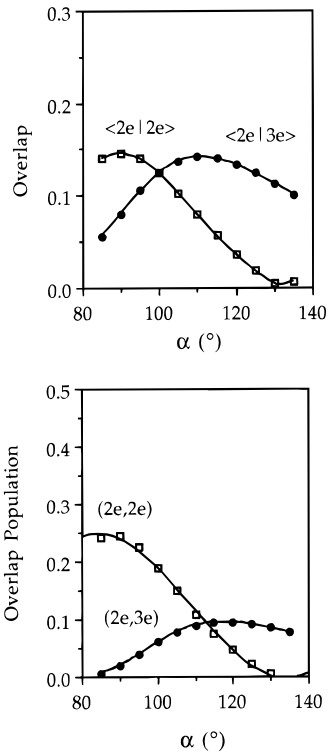

Figure 6. Pyramidality dependence of the overlap integral (top) and overlap population (bottom) between the e-type orbitals of the WH_4 fragments in the model compound $[W_2H_8]^{2-}$.

and, when combined, give rise to the parabollic behavior of the bond strength found in Figures 3 and 4.

In summary, the pyramidality dependence of the M−M bond lengths in the triply bonded M_2L_6 complexes is expected to be inverse, with a turnover point at ≈103° as a result of the symmetry-imposed variation of the hybridization of the π orbitals.

Structural Correlations

In order to confirm the above theoretical predictions, we have carried out a structural database search for M_2L_6 compounds of Mo and W (see Appendix for details). The retrieved structures were classified into families of compounds having

(12) Albright, T. A.; Burdett, J. K.; Whangbo, M.-H. *Orbital Interactions in Chemistry*; Wiley: New York, 1985.
(13) Chisholm, M. H.; Cotton, F. A.; Frenz, B. A.; Reichert, W. W.; Shive, L. W.; Stults, B. R. *J. Am. Chem. Soc.* **1976**, *98*, 4469.
(14) Blatchford, T. P.; Chisholm, M. H.; Huffman, J. C. *Inorg. Chem.* **1987**, *26*, 1920.
(15) Coffindaffer, T. W.; Rothwel, l. I. P.; Huffman, J. C. *Inorg. Chem.* **1983**, *22*, 2906.
(16) Chisholm, M. H.; Cotton, F. A.; Murillo, C. A.; Reichert, W. W. *Inorg. Chem.* **1977**, *16*, 1801.
(17) Gilbert, T. M.; Landes, A. M.; Rogers, R. D. *Inorg. Chem.* **1992**, *31*, 3438.
(18) Budzichowski, T. A.; Chacon, S. T.; Chisholm, M. H.; Feher, F. J.; Strib, W. *J. Am. Chem. Soc.* **1991**, *113*, 689.
(19) Chisholm, M. H.; Cotton, F. A.; Extine, M. W.; Stults, B. R. *J. Am. Chem. Soc.* **1976**, *98*, 4477.
(20) Chisholm, M. H.; Clark, D. L.; Folting, K.; Huffman, J. C. *Angew. Chem., Int. Ed. Engl.* **1986**, *25*, 1014.
(21) Chisholm, M. H.; Folting, K.; Hampden-Smith, M.; Smith, C. A. *Polyhedron* **1987**, *6*, 1747.
(22) Chisholm, M. H.; Parkin, I. P.; Folting, K.; Lubkovsky, E. B.; Streib, W. E. *J. Chem. Soc., Chem. Commun.* **1991**, 1673.
(23) Heppert, J. A.; Dietz, S. D.; Boyle, T. J.; Takusagawa, F. *J. Am. Chem. Soc.* **1989**, *111*, 1503.
(24) Chisholm, M. H.; Folting, K.; Haubrich, S. T.; Martin, J. D. *Inorg. Chim. Acta* **1993**, *213*, 17.
(25) Chisholm, M. H.; Cook, C. M.; Huffman, J. C.; Streib, W. E. *J. Chem. Soc., Dalton Trans.* **1991**, 929.
(26) Parkin, I. P.; Folting, K. *J. Chem. Soc., Dalton Trans.* **1992**, 2343.
(27) Chisholm, M. H.; Cotton, F. A.; Extine, M.; Millar, M.; Stults, B. R. *Inorg. Chem.* **1976**, *15*, 2244.
(28) Chisholm, M. H.; Hampden-Smith, M. J.; Huffman, J. C. *J. Am. Chem. Soc.* **1988**, *110*, 4070.
(29) Schulz, H.; Folting, K.; Huffman, J. C.; Streib, W. E.; Chisholm, M. H. *Inorg. Chem.* **1993**, *32*, 6056.
(30) Chisholm, M. H.; Eichhorn, B. W.; Folting, K.; Huffman, J. C. *Inorg. Chim. Acta* **1988**, *144*, 193.

Table 1. M−M Distances (Å), Average Pyramidality (α), and Internal Rotation (τ) Angles (deg) in Triple-Bonded M_2L_6 Complexes (M = Mo, W)

compound	τ	d_{M-M}	a	refcode	ref
$[Mo_2(NMe_2)_6]$	60.0	2.211	103.6	hxmamo10	13
$[Mo_2(NMe_2)_6]$	60.0	2.217	103.8	hxmamo10	13
$[Mo_2(Me_4en)_3]^a$	11.7	2.190	101.9	meammo10	14
$[Mo_2(O^iPr)_2(OMe_2Ph)_4]$	60.0	2.249	103.9	cawhox	15
$[Mo_2(O^iPr)_2(OMe_2Ph)_4]$	60.0	2.241	103.6	cawhox	15
$[Mo_2(O\text{-}2,2\text{-}Me_2Pr)_6]$	60.0	2.221	103.1	nepxmo10	16
$[Mo_2(O\text{-}\{CF_3\}_2\{CH_3\})_6]$	60.0	2.230	98.1	kulvoc	17
$[Mo_2(Si_7O_{12}Cy_7)_2]$	60.0	2.221	101.2	vingaa	18
$[Mo_2(Si_7O_{12}Cy_7)_2]$	60.0	2.209	100.5	vingaa	18
$[W_2(Me_4en)_3]^a$	11.8	2.265	101.6	fimdua	14
$[W_2(NMe_2)_6]$	60.0	2.290	103.1	hmamdw	19
$[W_2(NMe_2)_6]$	60.0	2.294	103.4	hmamdw	19
$[W_2(NMe_2)_6]$	59.9	2.294	103.8	admadw10	19
$[W_2(O^iPr)_6]$	60.0	2.315	106.7	fighos	20
$[W_2(\mu\text{-pinacolato-}O,O')_3]^a$	10.3	2.274	99.6	fummab	21
$[W_2(O\text{-Cy})_6]$	60.0	2.339	107.3	fummef	21
$[W_2(\mu\text{-}C_8H_{18}\text{-}O,O')_3]^a$	40.9	2.366	110.1	kolmut	22
$[W_2(O\text{-}^tBu)_4(\mu\text{-}C_{22}H_{16}\text{-}O,O')]^a$		2.324	103.6	vajhod	23
$[W_2(O\text{-}^tBu)_4(O\text{-}BMes_2)_2]$	2.9	2.352	104.3	hehnud	24
$[W_2(O\text{-}^tBu)_4(O\text{-}BMes_2)_2]$	12.5	2.326	108.8	hehnud	24
$[W_2(O\text{-}Si\{^tBuMe_2\})_6]$	60.0	2.325	100.6	jikvoo	25
$[W_2(O\text{-}2\text{-}^iPr\text{-}5\text{-MeCy})_6]$	22.2	2.338	103.8	vuhluf	26
$[W_2(O\text{-}2\text{-}^iPr\text{-}5\text{-MeCy})_6]$	41.9	2.337	105.2	vuhluf	26
$[W_2(NMe_2)_4Me_2]$		2.291	103.4	dmeamw	27
$[W_2(NMe_2)_4(2\text{-}MeC_3H_5)_2]$		2.286	102.7	gejsuj	28
$[W_2(NMe_2)_4(\mu\text{-Fc})]$		2.289	102.0	leflox	29
$[W_2(NMe_2)_4(\mu\text{-Fc})]$		2.289	102.3	leflox	29
$[W_2(NMe_2)_4\{CH(SiMe_3)_2\}_2]$		2.320	104.8	sudroy	30

[a] Bridging ligand.

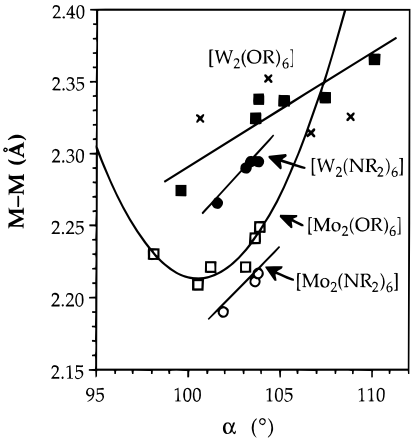

Figure 7. M−M bond distances plotted as a function of the average pyramidality angle α for compounds of the families $[Mo_2(NR_2)_6]$ (open circles), $[W_2(NR_2)_6]$ (filled circles), $[Mo_2(OR)_6]$ (open squares), and $[W_2(OR)_6]$ (filled squares). Least-squares lines through the experimental data are shown to illustrate the trends.

the same metal atoms and analogous ligands, and the two geometrical parameters, M−M distance and average M−M−L angle α, were calculated in the search for possible correlations (Table 1). The structural data for the $[M_2(NR_2)_6]$ and $[M_2(OR)_6]$ families (M = Mo, W) are plotted in Figure 7. In general, for angles α > 100°, the M−M distances increase with increasing pyramidalities, in contrast with the most common pattern shown by hundreds of complexes, in which the distances decrease with increasing α,[3,5,6] but which has some precedent in the families of amido and alkyl complexes of W_2L_8 stoichiometry with triple W−W bonds, and in the propyldiphosphine derivatives of Mo with quadruple Mo−Mo bonds, included in Table 2 for comparison. The inverted linear dependence found for the amido and alkoxo complexes of Mo(III) and W(III) (Figure 7) in the range of experimental pyramidalities is in excellent agreement with the above theoretical results. A remarkable feature of the Mo alkoxo complexes is that a parabolic behavior is apparently found, with a turnover point at α ≈ 100.6°. For the other three families, only the inverted region is observed. A word of caution must be said, however: in each of these three families, the structure with the shortest bond distance corresponds to a compound with the eclipsed conformation forced by a bridging ligand. The family of alkoxo W(III) complexes shows larger dispersion from the general trend. Hence, the trends found in the present work should be taken with caution and checked against the structural results for new compounds. The synthesis of compounds in these families covering a larger range of angles and distances therefore constitute a highly interesting experimental target.

In Table 2 we show the parameters for the least-squares fitting of the structural data for large α values to linear expressions of the type $d = b + c(\cos \alpha)$, which provide two interesting parameters: the *intrinsic* metal−metal bond distance (*b*), corresponding to planar ML_n fragments (i.e., α = 90°), and the *susceptibility to pyramidalization*, *c*. A good correlation between *d* and α is found for the amido complexes of Mo and W, and a somewhat poorer correlation for the alkoxo derivatives of the same metals (the structures marked with a cross was disregarded for the least-squares fitting). Comparison of the least-squares parameters of the compounds under study reveals two trends: (i) the intrinsic W−W bond distance is larger than the Mo−Mo one for the same set of ligands, and (ii) the susceptibility to pyramidalization is similar for the Mo and W compounds with the same set of ligands and larger for the amido than for the alkoxo ligands. In fact, the absolute value of the susceptibility to pyramidalization (*c*, Table 2) is largest for the compounds with amido ligands than for any other set of ligands, with the exception of the bridging carboxylato and analogous ligands.

Notice that all of the experimental values of α for the alkoxo and amido complexes of Mo (Table 2) are close to the calculated energy minima. At this point it is clear that the dependence of the metal−metal distance on the degree of pyramidalization is in general parabolic. However, only part of that curve is

Table 2. Structural Correlation Parameters for Several Families of Dinuclear M_2L_6 and M_2L_8 Complexes of Mo and W with M−M Multiple Bonds

M	L	bond order	*b*	*c*	*r*	d_{min}	d_{max}	α_{min}	α_{max}	σ (Å)	*N*
					M_2L_6						
Mo	NR_2	3	2.026	−0.793	0.993	2.190	2.217	101.9	103.8	0.010	3
Mo	OR	3	2.109	−0.551	0.873	2.209	2.249	100.5	103.9	0.012	5
W	NR_2	3	2.098	−0.836	0.979	2.265	2.294	101.6	103.8	0.008	4
W	OR	3	2.209	−0.469	0.929	2.274	2.366	99.6	110.1	0.025	6
					M_2L_8						
Mo	RCOO, RCONR′	4	2.158	1.774	0.845	2.062	.149	1.39	3.00	.0096	2
Mo	X, PR_3	4	2.191	0.197	0.874	2.12	2.16	102.8	109.3	0.004	7
Mo	RCOO, PR_3	4	2.131	0.189	0.945	2.09	2.12	94.2	101.0	0.003	21
W	RCOO, RCONR′	4	2.222	1.873	0.878	2.16	2.24	89.9	92.1	0.013	13
Mo	$R_2P(CH_2)_3PR_2$	4	1.997	−0.568	0.942	2.13	2.16	103.0	106.4	0.005	6
W	NR_2	3	2.007	−1.536	0.997	2.29	2.33	100.6	104.5	0.001	5
W	(LL)R	3	2.188	−0.466	0.985	2.19	2.30	90.2	105.2	0.008	8

[a] *b* and *c* are the least-squares parameters for the linear equation $d = b + c\cos(\alpha)$, *r* is the regression coefficient, σ is the standard deviation of the estimate, d_{min} and d_{max} represent the extreme values for the experimental distances in each data set and similarly for α_{min} and α_{max}; *N* is the number of structural data sets.

energetically attainable and, depending on where is the minimum, a normal (small angles) or an inverted (large angles) pyramidality effect appears. Of course, the presence of bridging ligands with a small bite strongly favors small angles, thus explaining the fact that complexes with carboxylato or analogous bridges always show a normal pyramidality effect (i.e., a positive value of the susceptibility *c*).[5] Bridges with larger bites, such as $R_2P(CH_2)_3PR_2$, allow for larger angles and show an inverted effect (negative susceptibility; see Table 2).

Finally, the pyramidality dependence of the W−W bond distances in the mixed-ligand complexes of general formula $W_2(NR_2)_4R'_2$ (presented in Table 1) apparently corresponds also with the expected parabolic behavior (regression coefficient 0.998), with a minimum distance (turnover point) at $\alpha \approx 102.6°$. However, given the relatively small number of compounds in this family, structural characterization of compounds with smaller bond angles should allow confirmation or disapproval of this interpretation of such data.

Acknowledgment. Financial support for this work was provided by DGICYT, Project PB92-0655. Allocation of computer time at the *Centre de Computació i Comunicacions de Catalunya* (*C*^{4}) was generously provided through a grant from FCR and Universitat de Barcelona. X.-Y.L. thanks CIRIT for a postdoctoral grant. The authors are indebted to E. Ruiz for many suggestions and technical advice and to F. Vilardell for help with the drawings.

Appendix

Searches in the Cambridge Structural Database[31] were carried out using version 5.11, covering entries up to Jan 17, 1996. A prospective search for compounds of Mo or W with the M_2L_6 stoichiometry and a triple M−M bond was first carried out. Afterward the search was restricted to those families which showed significative members.

The extended Hückel molecular orbital calculations[32] were carried out with the CACAO[33] and YAEHMOP[34] programs, using the modified Wolfsberg−Helmholz formula[35] and standard atomic parameters.[7,32,36] The following bond distances were used and kept constant throughout: W−W = 2.36 Å; W−H = 1.732 Å.

DFT calculations were carried out with the GAUSSIAN94 program[37] using the Slater exchange functional[38] with the generalized gradient correction given by Becke[39] and the correlation functional of Lee, Yang, and Parr.[40] The Hay−Wadt basis set was used, with a double-ζ quality for the valence and outermost core s and p orbitals, and effective core pseudopotentials for the inner shells.[41,42] As a check, we calculated the $d(\alpha)$ behavior of $[Os_2Cl_8]^{2-}$, which was in good qualitative agreement with that previously reported at the CASSCF level,[5] although the calculated distances were consistently longer by ∼0.1 Å in the present DFT calculations. For $[Mo_2(OH)_6]$ the following average bond distances and angles from the experimental structure of $[Mo_2(OCH_3\text{-}CMe_3)_6]$ were used: Mo−O = 0 1.88 Å; O−H = 0.958 Å; Mo−O−H = 109°. For $[Mo_2(NH_2)_6]$ the following parameters, taken from the structure of $[Mo_2(NMe_2)_6]$, were used: Mo−N = 1.98 Å; N−H = 0.975 Å, Mo−N−H1 = 116.3°; Mo−N−H2 = 133.4°. For $[Mo_2(OH)_4(NH_2)_2(NH_3)_2]$, the data were taken from the crystal structure of $[Mo_2(O^tBu)_4(PhNH)_2(PhNH_2)_2]$ as follows: Mo−N1 ($PhNH_2$) = 2.374 Å; Mo−N2 (PhNh) = 1.973 Å; Mo−O = 1.954 Å; N1−H = 0.957 Å; N2−H = 0.975 Å; O−H = 0.958 Å; Mo−N1−H = 119°; Mo−N2−H = 120°; Mo−O−H = 110°. For M_2L_6 complexes a staggered conformation was used throughout, according to the conformation found in most of the experimental structures (Table 1) and predicted to be more stable in previous theoretical studies.[8] For the M_2L_8 ones the eclipsed conformation was adopted, since the conformation on the M−M bonds in this family of compounds has been previously reported.[5]

IC9612358

(31) Allen, F.; Kennard, O.; Taylor, R. *Acc. Chem. Res.* **1983**, *16*, 146.
(32) Hoffmann, R. *J. Chem. Phys.* **1963**, *39*, 1397.
(33) Mealli, C.; Proserpio, D. *J. Chem. Educ.* **1990**, *67*, 399.
(34) Landrum, G. *YAeHMOP (Yet Another extended Hückel Molecular Orbital Package)* (Revision 1.2), Cornell University: Ithaca, NY, 1995.
(35) Ammeter, J. H.; Bürgi, H.-B.; Thibeault, J. C.; Hoffmann, R. *J. Am. Chem. Soc.* **1978**, *100*, 3686.
(36) Summerville, R. H.; Hoffmann, R. *J. Am. Chem. Soc.* **1976**, *98*, 7240.
(37) Frisch, M. J.; Trucks, G. W.; Schlegel, H. B.; Gill, P. M. W.; Johnson, B. G.; Robb, M. A.; Cheeseman, J. R.; Keith, T. A.; Petersson, G. A.; Montgomery, J. A.; Raghavachari, K.; Al-Laham, M. A.; Zakrzewski, V. G.; Ortiz, J. V.; Foresman, J. B.; Cioslowski, J.; Stefanov, B.; Nanayakkara, A.; Challacombe, M.; Peng, C. Y.; Ayala, P. Y.; Chen, W.; Wong, M. W.; Andres, J. L.; Replogle, E. S.; Gomperts, R.; Martin, R. L.; Fox, D. J.; Binkley, J. S.; Defrees, D. J.; Baker, J. P.; Stewart, J. P.; Head-Gordon, M.; Gonzalez, C.; Pople, J. A. *Gaussian 94* (Revision C.3); Gaussian, Inc.: Pittsburgh, PA, 1995.
(38) Slater, J. C. *The Self-Consistent Field for Molecules and Solids*; McGraw-Hill: New York, 1974.
(39) Becke, A. D. *Phys. Rev. A* **1988**, *38*, 3098.
(40) Lee, C.; Yang, W.; Parr, R. G. *Phys. Rev. B* **1988**, *37*, 785.
(41) Hay, P. J.; Wadt, W. R. *J. Chem. Phys.* **1985**, *82*, 270, 299.
(42) Wadt, W. R.; Hay, P. J. *J. Chem. Phys.* **1985**, *82*, 284.